ISSN: 1410-8917
Jurnal Kimia Sains & Aplikasi
e-ISSN: 2597-9914

Jurnal Kimia Sains dan Aplikasi 28 (6) (2025): 307-315

Jurnal Kimia Sains dan Aplikasi
Journal of Scientific and Applied Chemistry

Journal homepage: http://ejournal.undip.ac.id/index.php/ksa

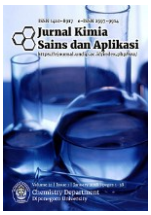

Synthesis and Characterization of Nickel(II) Imprinted Polymers as a Selective Adsorbent for Nickel(II) Ions

Siska Ela Kartika [1,*], Putri Septiani Hariyanto [1], Armeida D. R. Madjid [1], Sonita Afrita Purba Siboro [2], Roni Sujarwadi [2]

[1] Department of Chemistry, Faculty of Science and Technology, Universitas Islam Negeri Maulana Malik Ibrahim, Malang, Indonesia
[2] Research Center for Polymer Technology, Research Organization for Nanotechnology and Materials, National Research and Innovation Agency, Tangerang Selatan, Indonesia

* Corresponding author: siskaelakartika@uin-malang.ac.id

https://doi.org/10.14710/jksa.28.6.307-315

Article Info

Article history:

Received: 28th February 2025
Revised: 08th July 2025
Accepted: 09th July 2025
Online: 05th August 2025

Keywords:
adsorption; ion imprinted polymer; nickel pollution; Ni(II)-IPs; selective adsorption

Abstract

The rapid expansion of nickel mining in Indonesia, driven by the growing demand for electric vehicle batteries, has raised concerns about the environmental and health impacts of nickel pollution. This study presents the synthesis and characterization of a highly selective adsorbent, Nickel(II) Imprinted Polymers (Ni(II)-IPs), for the monitoring and removal of Ni(II) ions. Ni(II)-IPs were synthesized using precipitation polymerization by imprinting the Ni(II)-8-hydroxyquinoline complex into a polymer matrix through the polymerization of methacrylic acid and ethylene glycol dimethacrylate. Successful imprinting and subsequent leaching of Ni(II) ions using HNO_3 were confirmed by FTIR, SEM, and EDX characterization. Adsorption studies revealed that Ni(II)-IPs exhibit a high adsorption capacity of 70.26 mg/g at pH 7 within a short contact time of 15 minutes. Moreover, Ni(II)-IPs demonstrated excellent selectivity towards Ni(II) ions in the presence of competing ions, with relative selectivity coefficients of 1.20, 1.24, and 1.31 for Ni(II)/Cu(II), Ni(II)/Co(II), and Ni(II)/Pb(II), respectively. These findings highlight the potential of Ni(II)-IPs as an efficient and selective adsorbent for monitoring and removing Ni(II) ions from complex aqueous matrices, thereby addressing growing concerns about nickel pollution in Indonesia and beyond.

1. Introduction

Indonesia, the country with the largest nickel reserves in the world, has experienced a significant increase in nickel mining activities driven by the escalating global demand, particularly in the electric vehicle battery industry. The International Energy Agency projects a minimum 65% increase in global nickel production by 2030, fueled by the growing need for stainless steel and electric vehicle batteries as part of the global energy transition. Indonesia is poised to supply approximately two-thirds of this demand and has entered into multiple contracts with foreign investors in nickel mining [1, 2]. However, this rapid expansion poses serious environmental challenges. Large-scale nickel mining has resulted in water pollution and disruption of marine ecosystems in regions such as Buli Bay and Weda Bay in East Halmahera, North Maluku, where ore dredging has caused seawater discoloration and threatened marine life. Similar impacts have been reported on Labengki and Kabaena Islands, Southeast Sulawesi, where mining sediments have increased water turbidity and led to declines in fish and seaweed populations. Beyond ecological damage, nickel exposure is linked to various health issues, including dermatological, cardiovascular, immunological, neurological, renal disorders, and cancers [2, 3]. This situation presents a dilemma between the demand for nickel to support green technologies and the imperative to mitigate environmental harm. The World Health Organization (WHO) has set a maximum permissible Ni(II) concentration of 0.07 mg/L in water, underscoring the need for effective environmental monitoring and remediation [4].

Analytical techniques such as Atomic Absorption Spectrophotometry (AAS) are commonly employed to determine nickel concentrations. However, AAS faces limitations in environmental matrices due to low sensitivity and matrix interferences, necessitating effective separation methods prior to analysis [5]. Various separation strategies, including liquid extraction, ion exchange, and solid phase extraction (SPE), have been explored for metal ion analysis [6]. Among these, SPE is preferred for its reduced solvent consumption, higher precision, and efficient analyte-matrix separation [7, 8]. Conventional adsorbents used in SPE, such as zeolite, silica, alumina, chitosan, and activated carbon, lack sufficient selectivity for specific metal ions, which limits their effectiveness in complex samples [9]. Therefore, selecting an adsorbent with high selectivity is critical for successful SPE applications.

Ion-imprinted polymers (IIPs) have emerged as promising selective adsorbents due to their ability to form specific cavities complementary to target metal ions. These cavities are generated by polymerizing functional monomers and crosslinkers in the presence of a metal ion template, which is subsequently removed to leave behind recognition sites matching the target ion's size, charge, coordination number, and geometry [10, 11]. This molecular imprinting approach enhances selectivity, making IIPs highly suitable for metal ion separation and detection.

Despite extensive research on IIPs, several gaps remain. While methacrylic acid (MAA) and ethylene glycol dimethacrylate (EGDMA) are widely used as monomer and crosslinker, respectively, the incorporation of 8-hydroxyquinoline—a ligand known for its strong chelating affinity toward Ni(II)—has been less explored in Ni(II)-IIPs. Additionally, many studies report slow adsorption kinetics or insufficient evaluation of selectivity against ions with similar properties, such as Co(II) and Cu(II). Fast adsorption kinetics are essential for practical environmental monitoring, yet this aspect is often underreported. Furthermore, comprehensive characterization linking the imprinting mechanism to adsorption performance remains limited.

To address these challenges, this study focuses on synthesizing Ni(II)-imprinted polymers using MAA and EGDMA in the presence of a Ni(II)-8-hydroxyquinoline complex. This approach leverages the strong ligand affinity of 8-hydroxyquinoline to enhance selective cavity formation and improve adsorption performance. The synthesized Ni(II)-IPs are characterized using FTIR, SEM, and EDX techniques. Batch adsorption experiments are conducted to evaluate the effects of pH, time, adsorption capacity, and selectivity under environmentally relevant conditions. By addressing the gaps in ligand selection, kinetics, and selectivity evaluation, this research aims to develop a highly selective, fast-acting adsorbent suitable for effective monitoring and removal of Ni(II) ions from contaminated water sources.

2. Experimental

2.1. Tools

The instruments and equipment used included standard laboratory glassware, an analytical balance, a magnetic stirrer, a hot plate, an oven, a pH meter, a Shimadzu Fourier Transform Infrared Spectrometer (FTIR), a JEOL JSM-6510 Scanning Electron Microscope coupled with Energy Dispersive X-ray (SEM-EDX), and a Varian AA240 Atomic Absorption Spectrometer (AAS).

2.2. Materials

The materials used in this study were $NiCl_2.6H_2O$ (Smartlab), 8-hydroxyquinoline (8-HQ, Himedia), ethanol (analytical grade), acetonitrile (analytical grade), methacrylic acid (MAA; Sigma Aldrich), ethylene glycol dimethacrylate (EGDMA; Sigma Aldrich), azobisisobutyronitrile (AIBN, Sigma Aldrich), HNO_3 (analytical grade), HCl (Merck), NaOH (Merck), $CoCl_2.6H_2O$ (Smartlab), $Cu(NO_3)_2$ (Merck), $Pb(NO_3)_2$ (Merck), nitrogen gas, filter paper, and distilled water.

2.3. Synthesis of Ni(II)-IPs

Ni(II)-IPs were synthesized using precipitation polymerization. The procedure involved reacting 0.0475 grams (0.2 mmol) of $NiCl_2.6H_2O$ with 0.0725 grams (0.5 mmol) of 8-hydroxyquinoline in a solvent mixture of 80 mL of ethanol and 40 mL of acetonitrile (2:1). The solution was stirred for 30 minutes. The solution was added with 0.7 mL (8 mmol) of methacrylic acid, 7.5 mL (40 mmol) of ethylene glycol dimethacrylate, and 1.2 mL (8 mmol) of azobisisobutyronitrile and then stirred for 30 minutes. The solution was cooled in the freezer for 30 minutes and flowed with nitrogen gas for 5 minutes. The mixture was put into an oven at 60°C for 8 hours. After being washed with 100 mL of ethanol, the polymer was dried in an oven at 60°C for an hour. The imprinted Ni(II) ions were removed by stirring the polymer in 2 M HNO_3 for 5 hours, after which the Ni(II)-IPs were dried again at 60°C. Non-imprinted polymers (NIPs) were prepared similarly but without the Ni(II)-8-hydroxyquinoline complex. The molar ratio of Ni(II): 8-hydroxyquinoline: MAA: EGDMA: AIBN was 2:5:80:400:80.

2.4. Effect of pH

The effect of pH was evaluated by contacting 0.02 g of Ni(II)-IPs with 25 mL of 5 ppm Ni(II) solution for 30 minutes at different pH values (4, 5, 6, 7, and 8). The filtrate was analyzed using AAS at a wavelength of 232.1 nm. The percentage of Ni(II) adsorption was calculated using Equation (1).

$$\%\ Ni(II)\ \text{adsorption} = \frac{(C_0 - C_e)}{C_0} \times 100\% \quad (1)$$

Where, C_0 and C_e are the initial and equilibrium concentrations of Ni(II), respectively.

2.5. Effect of Contact Time

The optimum contact time was determined by contacting 0.02 g of Ni(II)-IPs with 25 mL of 5 ppm Ni(II) solution at the optimum pH for varying durations of 5, 10, 15, 30, 45, and 60 minutes. The filtrate was analyzed using AAS at a wavelength of 232.1 nm.

2.6. Determination of Adsorption Capacity

To determine adsorption capacity, 0.02 g of Ni(II)-IPs and NIPs were contacted with 25 mL of Ni(II) solution at optimum pH and contact time, using concentrations of 20, 50, 80, and 100 ppm. The filtrate was analyzed by AAS at 232.1 nm. Adsorption capacity was calculated using Equation (2).

$$Q_e = \frac{(C_0 - C_e)\,V}{W} \quad (2)$$

Where, W indicates the mass of Ni(II)-IPs, V is the volume of Ni(II), Q_e is the amount of Ni(II) adsorbed by Ni(II)-IPs, C_0 is the initial concentration of Ni(II), and C_e is the concentration of Ni(II) at equilibrium.

2.7. Determination of Selectivity

Selectivity was evaluated by contacting 0.025 g of Ni(II)-IPs and NIPs with 30 mL of mixed metal ion solutions—Ni(II)/Co(II), Ni(II)/Cu(II), and Ni(II)/Pb(II)—each at 10 ppm concentration. After filtration, the filtrate was analyzed by AAS at wavelengths of 283.3 nm (Pb), 240.7 nm (Co), 324.8 nm (Cu), and 232.1 nm (Ni). The distribution coefficient (K_d), selectivity coefficient (K), and relative selectivity coefficient (K') were calculated using Equations (3-5).

$$K_d = \frac{Q_e}{C_e} \quad (3)$$

$$K = \frac{K_d Ni(II)}{K_d M} \quad (4)$$

$$K' = \frac{K\ Ni(II)-IPs}{K\ \text{NIPs}} \quad (5)$$

Where, Q_e is the amount of Ni(II) adsorbed by Ni(II)-IPs, C_e is the concentration of Ni(II) at equilibrium, and M is the competitive metal ions.

3. Results and Discussion

3.1. Synthesis of Ni(II)-IPs

The synthesis of Ni(II)-IPs consisted of three stages. The first step was the formation of the Ni(II)-8-HQ complex; second, polymerization between the Ni(II)-8-HQ complex with MAA and EGDMA; and third, the removal of Ni(II) from the polymer matrix using 2 M HNO_3. The ligand 8-HQ was a bidentate metal chelator with oxygen donor atoms in the hydroxyl group and nitrogen in its cyclic chain. The donor atom 8-HQ would bond with first-row transition metals that have empty d orbitals, such as nickel (Ni) [12].

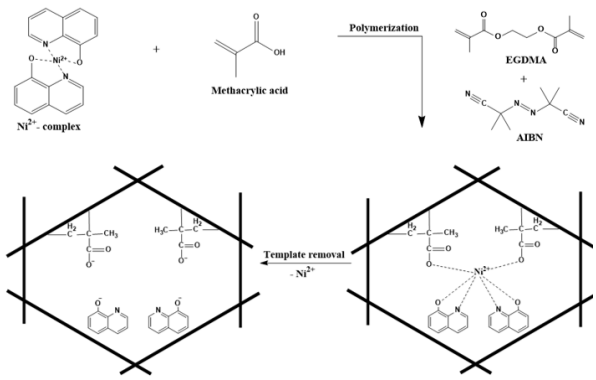

Figure 1. Proposed mechanism of Ni(II)-IPs

MAA was a monomer utilized to keep the polymer matrix stable during the printing process [13]. Monomers were determinants of the strength and weakness of the interaction of Ni(II)-IPs with the Ni(II) ions. MAA formed a dimerization reaction, thereby increasing the polymer imprinting effect [14]. EGDMA was a cross-linking agent that serves as a backbone to control the shape of the polymer matrix, maintain cavity stability after Ni(II) is removed from the polymer matrix, and preserve mechanical stability [13, 15]. EGDMA has an allyl functional group that can cross-link with MAA and produce stable and rigid Ni(II)-IPs [16, 17].

Azobisisobutyronitrile was an initiator that functions to initiate the polymerization process [18]. Polymerization was divided into initiation, propagation, and termination stages [19]. In the initiation stage, free radicals are formed and react with methacrylic acid monomers to produce monomer radicals, which initiate chain growth. Propagation involves the continuous addition of monomers to form polymers, while termination occurs when the monomer supply is depleted [20]. Ethanol would dissolve residues such as unreacted reactants trapped in the polymer matrix. Ni(II) ions were removed from the polymer matrix to form a cavity that has a memory effect on Ni(II) ions. The memory effect was formed due to the similarity of size, charge, geometry, and coordination number between the cavity and the Ni(II). A cavity in the polymer matrix can improve Ni(II)-IPs' selectivity [11].

The synthesized Ni(II)-IPs were obtained as a homogeneous white powder with a smooth, dry texture, and no agglomeration was observed. The yields of Ni(II)-IPs and NIPs were 76.21% and 83.85%, respectively, calculated based on the total weight of the starting materials. The slightly lower yield for Ni(II)-IPs is attributed to material loss during the template leaching process. Figure 1 illustrates that Ni(II) ions bind to the donor atoms O and N in 8-hydroxyquinoline, forming the Ni(II)-8-hydroxyquinoline complex [21]. During polymerization, covalent bonds are formed between MAA and EGDMA [13], in which the allyl group of EGDMA reacts with the C=C conjugated C=O group of MAA [17].

3.2. Characterization of Ni(II)-IPs

3.2.1. FTIR Characterization

The success of the synthesis of Ni(II)-IPs was indicated by the disappearance of the "C=C conjugated C=O" vibration and the emergence of C=O stretching and C-O stretching vibrations (Figure 2). The "C=C conjugated C=O" vibration in MAA appeared at 1690.06 cm^{-1}. The vibration of "C=C conjugated C=O" appeared at 1693.38 cm^{-1} [22]. The vibration of C=O stretching appeared at 1717.16, 1721.44, and 1722.86 cm^{-1}, while the vibration of C-O stretching appeared at 1142.40, 1148.10, and 1146.67 cm^{-1}. The vibration of C=O stretching appeared at 1725-1705 cm^{-1} [23]. The vibration of C-O stretching appeared at 1260-1000 cm^{-1} [24]. The disappearance of the vibration of C=C conjugated C=O and the emergence of C=O stretching and C-O stretching vibrations indicated that polymerization between MAA and EGDMA has formed [22].

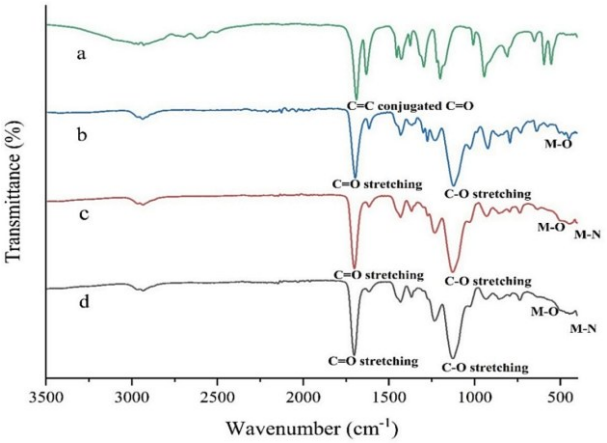

Figure 2. FTIR spectra of (a) MAA, (b) NIPs, (c) Ni(II)- IPs before leaching, (d) Ni(II)-IPs after leaching

M-N vibrations in Ni(II)-IPs before leaching and Ni(II)-IPs after leaching appeared at 452.10 and 453.53 cm^{-1}. M-N vibrations appeared at 451-461 cm^{-1} [25]. M-O vibrations in Ni(II)-IPs before leaching appeared at 526.27 cm^{-1}. M-O vibrations in NIPs and Ni(II)-IPs after leaching appeared at the same wave number, namely 527.69 cm^{-1}. M-O vibrations appeared at 525-599 cm^{-1} [25]. The occurrence of wave number shifts in M-N and M-O vibrations in Ni(II)-IPs before leaching and Ni(II)-IPs after leaching indicated that Ni(II) could be released from the polymer matrix using 2 M HNO_3.

3.2.2. SEM Characterization

SEM analysis was performed to investigate the surface morphology of NIPs, Ni(II)-IPs before leaching, and Ni(II)-IPs after leaching, as shown in Figure 3. The Ni(II)-IPs exhibited a noticeably rougher surface texture with aggregate formation compared to the smoother, more homogeneous, and denser surface of the NIPs, which showed limited porosity. After the leaching process, the Ni(II)-IPs displayed enhanced porosity relative to both NIPs and pre-leached Ni(II)-IPs [21]. The rougher and more porous morphology of Ni(II)-IPs provides clear evidence of the successful imprinting process. This increased surface roughness arises from the removal of Ni(II) ions during leaching, which creates selective binding cavities tailored for Ni(II) ions. These cavities possess specific shapes, sizes, geometries, and coordination numbers complementary to Ni(II), enabling selective rebinding.

The formation of these cavities not only increases the number of accessible active sites but also enhances the overall surface area, both of which are critical for improving the adsorption capacity and selectivity of the polymer. The leaching process effectively opens binding sites previously occupied by the Ni(II) template ions, thereby increasing the porosity and accessibility of the polymer surface. Ni(II) ions initially form complexes with 8-hydroxyquinoline ligands and become embedded within the hardened polymer matrix during synthesis. The efficiency of the leaching process directly influences the number of available binding sites and consequently the porosity of the material, which in turn positively impacts adsorption efficiency.

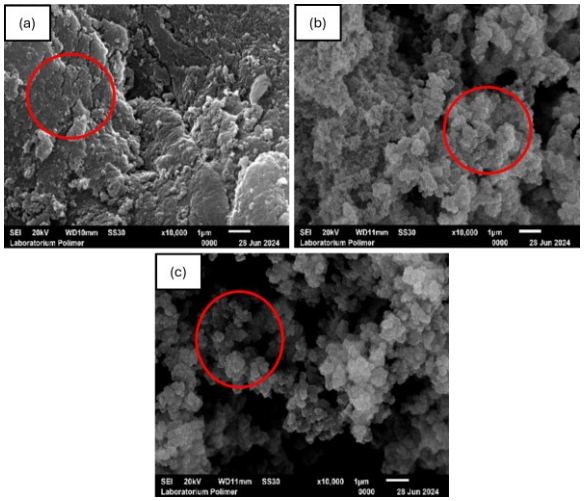

Figure 3. SEM images of (a) NIPs, (b) Ni(II)-IPs before leaching, and (c) Ni(II)-IPs after leaching

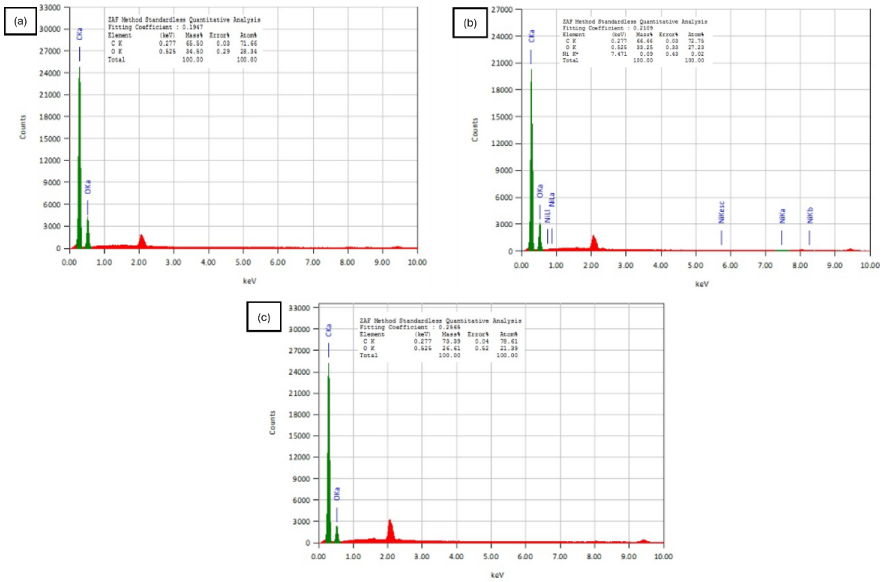

Figure 4. EDX spectra of (a) NIPs, (b) Ni(II)-IPs before leaching, and (c) Ni(II)-IPs after leaching

3.2.3. EDX Characterization

EDX characterization was conducted to determine the elemental composition of the polymer. The analysis confirmed the presence of carbon, oxygen, and nickel in the polymer, as shown in Figure 4. Ni(II)-IPs before leaching contained 0.09 mass% Ni(II), whereas no nickel was detected in the Ni(II)-IPs after leaching. The absence of Ni(II) in the leached samples confirms the successful removal of nickel ions from the polymer matrix.

3.3. Effect of pH

The batch method was used to investigate the effect of pH on Ni(II) adsorption within the pH range of 4 to 8, as shown in Figure 5. The adsorption capacity of Ni(II)-IPs increased steadily from pH 4 to pH 7, after which a slight decrease was observed at pH 8. At lower pH values, Ni(II) adsorption was less effective due to the high concentration of H^+ ions, which compete with Ni(II) for binding sites on the Ni(II)-IPs, thereby reducing the adsorption capacity [26]. Besides, Hu *et al.* [27] stated that at pH values below pH 7, the nitrogen atom in 8- hydroxyquinoline becomes protonated, leading to a decrease in Ni(II) adsorption. At pH values higher than 7, Ni(II)-IPs adsorption slightly declined. This is due to the presence of OH^- in the solution, resulting in precipitation due to the formation of $Ni(OH)_2$ hydroxide. The ideal pH for Ni(II) adsorption on ion-imprinted polymers-silica gel, Ni-Cu IIP, and ion-imprinted polymers-acrylamide is 7, according to several studies [28, 29, 30].

3.4. Effect of Contact Time

Using the batch method, the influence of contact time on the adsorption of Ni(II) was examined at times of 5, 10, 15, 30, 45, and 60 minutes, as shown in Figure 6. The adsorption of Ni(II) on Ni(II)-IPs reached its optimum at 15 minutes, after which the percentage of adsorbed Ni(II) remained nearly constant. Therefore, extending the contact time beyond 15 minutes was ineffective in increasing the adsorption capacity, as the Ni(II)-IPs had become saturated with Ni(II) ions [31]. This shows a better performance as a Ni(II) adsorbent, achieving maximum adsorption within a relatively short time [31, 32].

3.5. Ni(II)-IPs Adsorption Capacity

The adsorption capacity, defined as the highest quantity of metal ions adsorbed per unit mass of polymer [6], was determined by contacting Ni(II)-IPs with Ni(II) solutions at concentrations of 20, 50, 80, and 100 ppm. These concentrations were selected to enable measurement of the maximum adsorption capacity while reflecting realistic conditions encountered in wastewater treatment. Additionally, this concentration range provides a suitable basis for adsorption isotherm modeling. It also allows for a meaningful evaluation of the efficiency and selectivity advantages of Ni(II)-IPs compared to NIPs. As shown in Figure 7, Ni(II)-IPs exhibit significantly higher adsorption capacity than NIPs.

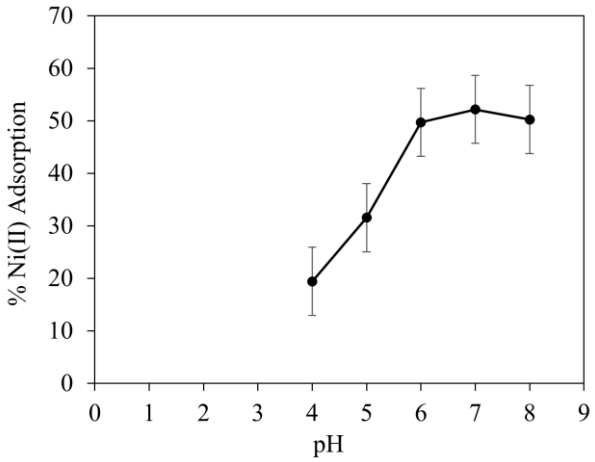

Figure 5. Effect of pH on Ni(II) adsorption percentage

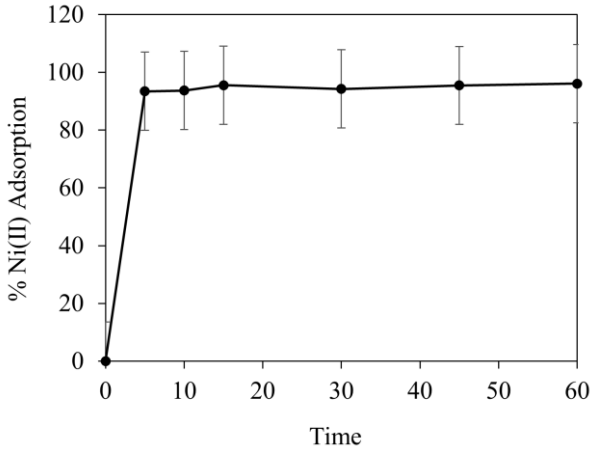

Figure 6. Effect of contact time on Ni(II) adsorption percentage

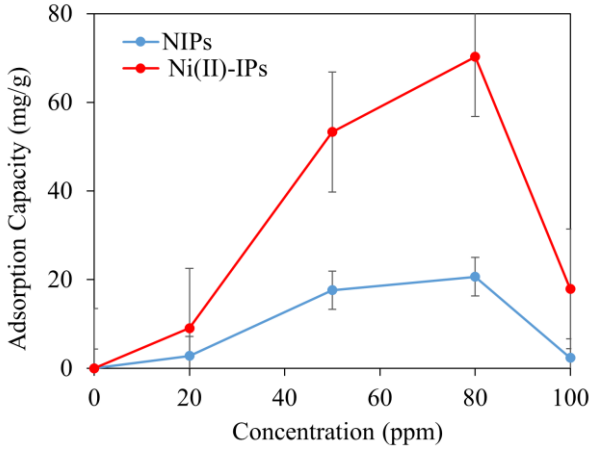

Figure 7. Adsorption capacity of Ni(II)-IPs and NIPs

Ni(II)-IPs had an adsorption capacity of 70.26 mg/g at pH 7 after 15 minutes. The adsorption capacity reaches its optimum level at 80 ppm and increases with increasing initial Ni(II) concentration. At concentrations above 80 ppm, the adsorption capacity decreased due to the saturation of the adsorbent, which reduced adsorption efficiency. Once the surface active sites of the adsorbent are fully occupied by metal ions, further increases in concentration do not enhance the adsorption capability [33].

Table 1. Selectivity of Ni(II)-IPs

Binary Solution	Metal ion	K_d NIPs	K_d Ni(II)-IPs	*K* NIPs	*K* Ni(II)-IPs	K'
Ni-Cu	Ni	0.54	4.22	0.22	0.26	1.20
	Cu	2.51	16.33			
Ni-Co	Ni	0.77	0.97	0.94	1.17	1.24
	Co	0.82	0.83			
Ni-Pb	Ni	0.64	2.13	0.21	0.28	1.31
	Pb	2.99	7.61			

3.6. Selectivity of Ni(II)-IPs

Ni(II) solution was mixed with Co(II), Cu(II), and Pb(II) solutions in order to determine selectivity using the batch method. Selectivity was assessed for 15 minutes at pH 7. As shown in Table 1, Ni(II)-IPs exhibited higher *K* values than NIPs. The *K*' values for Ni(II)/Cu(II), Ni(II)/Co(II), and Ni(II)/Pb(II) were 1.20, 1.24, and 1.31, respectively. A *K*' value above 1 indicates good selectivity for Ni(II) ions [34]. This enhanced selectivity arises from the imprinted cavities in Ni(II)-IPs, which are complementary to Ni(II) in terms of size, charge, geometry, and coordination number [11]. In this study, interfering ions with similar size and charge characteristics to Ni(II), such as Cu(II), Co(II), and Pb(II), were used to evaluate selectivity under strong competitive conditions.

The metal radii of Ni(II), Co(II), Cu(II), and Pb(II) are 0.069, 0.065, 0.073, and 0.119 Å, respectively. A greater difference between the ionic radius of Ni(II) and that of the competing metal results in a higher *K*' value due to the mismatch with the Ni(II)-IPs cavities [28]. These cavities are specifically tailored to the size and geometry of Ni(II) ions (0.069 Å). When the ionic radius of an interfering ion is similar to that of Ni(II), such as Co(II) and Cu(II), these ions can partially fit into the cavities, resulting in lower selectivity (lower *K*' values). Conversely, Pb(II) has a significantly larger ionic radius (difference Δr = 0.050 Å) and does not fit well into the cavities, leading to a higher *K*' value and greater selectivity for Ni(II). Thus, the selectivity of Ni(II)-IPs is strongly influenced by the size compatibility between the imprinted cavities and the ionic radii of competing ions.

Selectivity arises from the precise compatibility of the cavity shape, with 8-hydroxyquinoline and the MAA monomer playing crucial roles. The 8-hydroxyquinoline ligand is used as a chelating agent with a strong affinity for Ni(II) during the printing process, forming a stable chelation complex that facilitates cavity formation. The presence of functional groups in the chelation complex and monomers in the polymer matrix increases the bond strength and selectivity.

Table 2 shows that Ni(II)-IPs have better performance compared to several other adsorbents. Ni(II)-IPs were effective for the adsorption of Ni(II) because it has high adsorption capacity and selectivity in a relatively short time (15 minutes). Ni(II)-IPs can be used as a good candidate for the adsorption of Ni(II) and have the potential to be applied for the adsorption of Ni(II) in environmental samples.

Table 2. Adsorption capacity and adsorption time of various adsorbents

Adsorbent	Adsorption capacity (mg/g)	Time (minutes)	Ref.
Ion-imprinted polymers-silica gel	20.30	12	[28]
Lycopersicum esculentum (tomato) leaf powder	58.82	105	[35]
Dolomite powder	1.70	105	[36]
Gram-positive bacteria (*Brevibacillus laterosporus*) (MTCC1628)	44.44	120	[37]
Chitosan modification	42.41	1260	[38]
Ni(II)-IPs	70.26	15	Current study

3.7. Adsorption Isotherms

In this study, the adsorption behavior of Ni(II) ions on Ni(II)-IPs was evaluated using both Langmuir and the Freundlich isotherm models. The Langmuir isotherm assumes monolayer adsorption on a homogeneous surface with identical binding sites, typically indicative of chemisorption. In contrast, the Freundlich isotherm describes adsorption on a heterogeneous surface with varying affinities, commonly associated with physisorption [39]. Figure 8 presents the linearized plots of both isotherms, with correlation coefficients (R^2) of 0.958 for Langmuir and 0.525 for Freundlich. The higher R^2 value for the Langmuir model indicates that it better describes the adsorption process of Ni(II) ions onto Ni(II)-IPs. This suggests that adsorption occurs predominantly as a monolayer on a homogeneous surface without significant interaction between adsorbed ions.

Furthermore, the adsorption mechanism is primarily chemisorption, which is supported by the formation of coordinate covalent bonds between the Ni(II) ions and the functional groups of the 8-hydroxyquinoline ligand. Moreover, the presence of specific cavities in the Ni(II)-IPs, created during the imprinting process, provides a "memory effect" for Ni(II) ions. This effect arises from the similarity in size, charge, geometry, and coordination number between the template Ni(II) ions and the imprinted sites, enhancing selective and efficient binding.

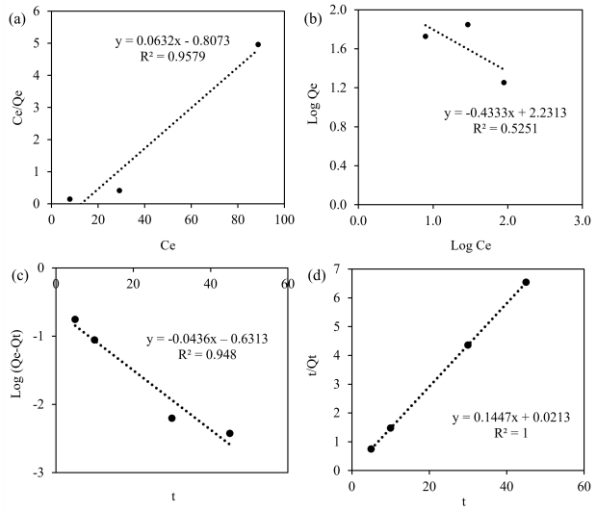

Figure 8. Isotherm and kinetics adsorption (a) Langmuir (b) Freundlich (c) Pseudo-first-order (d) Pseudo-second-order

3.8. Adsorption Kinetics

The adsorption kinetics of Ni(II) ions onto Ni(II)-IPs were analyzed using both pseudo-first-order and pseudo-second-order kinetic models. The R^2 values obtained from the linearized plots (Figure 8) were 0.948 for the pseudo-first-order and 1.000 for the pseudo-second-order model. The higher R^2 value for the pseudo-second-order model indicates a better fit, suggesting that the adsorption process is primarily controlled by chemisorption [39, 40]. This confirms that Ni(II) ions are adsorbed onto the surface of Ni(II)-IPs through chemical interactions involving electron sharing or exchange.

4. Conclusion

In this study, Ni(II)-IPs were successfully synthesized using methacrylic acid (MAA), EGDMA, Ni(II), and 8-hydroxyquinoline as monomers, crosslinkers, templates, and ligands. FTIR, SEM, and EDX characterizations confirmed the successful synthesis of Ni(II)-IPs and the successful leaching process of Ni(II) from the polymer matrix. The adsorption capacity of Ni(II)-IPs was 70.26 mg/g at pH 7 in a relatively short time (15 minutes). The relative selectivity coefficient (K') values of Ni(II)/Cu(II), Ni(II)/Co(II), and Ni(II)/Pb(II) were 1.20, 1.24, and 1.31, respectively. These results show that even when matrix interference is present, Ni(II)-IPs remain selective for Ni(II) ions. Future studies could focus on the monitoring of nickel in real environmental water samples.

Acknowledgement

We would like to thank the State Islamic University of Maulana Malik Ibrahim Malang, especially the Analytical Chemistry Research Group, and the National Research and Innovation Agency, especially the Polymer Technology Research Center, for their assistance and support in this research.

References

[1] Valdya Baraputri, Lingkungan di Sulawesi Tenggara terancam limbah tambang nikel - 'Yang kamu rusak adalah masa depannya', BBC News Indonesia, 2023

[2] Yusuf Wahil, Victoria Milko, Global demand spurring Indonesia's mining boom comes at a cost for many communities, AP News, 2024

[3] Muhammad Aris, Tamrin A. Ibrahim, Lidiawati Nasir, Kontaminasi logam nikel (Ni) pada struktur jaringan ikan, Budidaya Perairan, 9, 1, (2021), 64-72 https://doi.org/10.35800/bdp.9.1.2021.31566

[4] A. Giove, Y. El Ouardi, A. Sala, F. Ibrahim, S. Hietala, E. Sievänen, C. Branger, K. Laatikainen, Highly selective recovery of Ni(II) in neutral and acidic media using a novel Ni(II)-ion imprinted polymer, Journal of Hazardous Materials, 444, (2023), 130453 https://doi.org/10.1016/j.jhazmat.2022.130453

[5] Suci Aprilia, Validasi Metode Penentuan Kadar Logam Zn dan Ni Menggunakan Spektrofotometri Serapan Atom (SSA) dalam Limbah Abu Layang di Puslabfor Polri Jakarta, Skripsi, Program Study DIII Analisis Kimia, Universitas Islam Indonesia, Yogyakarta, 2022

[6] Siska Ela Kartika, Muhammad Bachri Amran, Sintesis dan Karakterisasi Poly (Anthranilic Acid-Co-Formaldehyde) untuk Adsorpsi Ion Pb(II), ALCHEMY: Journal of Chemistry, 9, 1, (2021), 15-25 https://doi.org/10.18860/al.v9i1.11476

[7] Tri Ulfa Rahmatia, Metode SPE (Solid Phase Extraction) sebagai Alternatif Terbaru dalam Analisis dan Pemurnian Senyawa Obat, Farmaka, 14, 2, (2017), 151-171

[8] Youssef El Ouardi, Alessio Giove, Markku Laatikainen, Catherine Branger, Katri Laatikainen, Benefit of ion imprinting technique in solid-phase extraction of heavy metals, special focus on the last decade, Journal of Environmental Chemical Engineering, 9, 6, (2021), 106548 https://doi.org/10.1016/j.jece.2021.106548

[9] Yuli Rohyami, Penentuan Cu, Cd dan Pb dengan AAS Menggunakan Solid Phase Extraction, Asian Journal of Innovation and Entrepreneurship (AJIE), 2, 01, (2013), 19-25

[10] Muhammad Cholid Djunaidi, Abdul Haris, Pardoyo Pardoyo, Rosdiana K, Pengaruh Jumlah Mol Kroslinker pada Selektifitas IIP Berbasis Polieugenol terhadap Fe(III), ALCHEMY Jurnal Penelitian Kimia, 14, 2, (2018), 290-302 https://doi.org/10.20961/alchemy.14.2.12426.291-302

[11] Keke Zhi, Jinwang Duan, Jiarui Zhang, Lianting Huang, Lianghui Guo, Lulu Wang, Progress and Prospect of Ion Imprinting Technology in Targeted Extraction of Lithium, Polymers, 16, 6, (2024), 833 https://doi.org/10.3390/polym16060833

[12] Eka Sulistya Hermawati, Suhartana Suhartana, Taslimah Taslimah, Sintesis dan Karakterisasi Senyawa Kompleks Zn(II)-8-Hidroksikuinolin, Jurnal Kimia Sains dan Aplikasi, 19, 3, (2016), 94-98 https://doi.org/10.14710/jksa.19.3.94-98

[13] Neli Kartika Asni, Maria Monica Sianita, Pengaruh Jumlah Crosslinker Terhadap Persen Ekstraksi pada Sintesis Molecularly Imprinted Polymer Sebagai Adsorben Untuk Kloramfenikol, Unesa Journal of Chemistry, 9, 3, (2020), 179-188 https://doi.org/10.26740/ujc.v9n3.p179-188

[14] Indraswari Pitaloka, Dika Pramita Destiani, Molecular Imprinting Solid Phase Extraction

Monomer Asam Metakrilat (MAA) Metode Ruah dan Endapan, Farmaka, 15, 2, (2017), 53-69

[15] Maria Monica Sianita, Trifena Meysia Yusuf, Pengaruh Jumlah Porogen pada Sintesis MIP (Molecularly Imprinted Polymer) Terhadap Adsorpsi MIP-Kloramfenikol, Unesa Journal of Chemistry, 11, 1, (2022), 53-60 https://doi.org/10.26740/ujc.v11n1.p53-60

[16] Hajriana Hajriana, Sintesis dan Karakterisasi Polimer Bercetakan Molekul Menggunakan Monomer Metil Metakrilat Kombinasi Pengikat Silang Etilen Glikol Dimetakrilat Sebagai Adsorben Untuk Molekul Dibutilftalat, Skripsi, Kimia, Universitas Hasanuddin, Makassar, 2022

[17] Agung Abadi Kiswandono, Synthesis and Performance Test of Co-Eegdma as a Carrier in Phenol Transport Using Polymer Inclusion Membrane, Jurnal Penelitian Saintek, 22, 2, (2018), 114-125

[18] Zhongqi Ren, Delong Kong, Keyuan Wang, Weidong Zhang, Preparation and adsorption characteristics of an imprinted polymer for selective removal of Cr(VI) ions from aqueous solutions, Journal of Materials Chemistry A, 2, 42, (2014), 17952-17961 https://doi.org/10.1039/C4TA03024A

[19] T. Pirman, M. Ocepek, B. Likozar, Radical Polymerization of Acrylates, Methacrylates, and Styrene: Biobased Approaches, Mechanism, Kinetics, Secondary Reactions, and Modeling, Industrial & Engineering Chemistry Research, 60, 26, (2021), 9347-9367 https://doi.org/10.1021/acs.iecr.1c01649

[20] Nadhrah Wivanius, Emil Budianto, Sintesis dan Karakterisasi Hidrogel Superabsorben Kitosan Poli(N-Vinilkaprolaktam) (Pnvcl) dengan Metode Full IPN (Interpenetrating Polymer Network), Pharmaceutical Sciences and Research, 2, 3, (2015), 5 https://doi.org/10.7454/psr.v2i3.3483

[21] Yasemin Işıkver, Sabri Baylav, Synthesis and characterization of metal ion-imprinted polymers, Bulletin of Materials Science, 41, 2, (2018), 49 https://doi.org/10.1007/s12034-018-1578-2

[22] T. Wirawan, G. Supriyanto, A. Soegianto, Synthesis, characterization, and application of novel Zn(II)-ionic imprinted polymer for preconcentration of Zn(II) ions from aqueous solution, IOP Conference Series: Materials Science and Engineering, 349, 1, (2018), 012064 https://doi.org/10.1088/1757-899X/349/1/012064

[23] D. A. Long, Infrared and Raman characteristic group frequencies. Tables and charts George Socrates John Wiley and Sons, Ltd, Chichester, Third Edition, 2001. Price £135, Journal of Raman Spectroscopy, 35, 10, (2004), 905 https://doi.org/10.1002/jrs.1238

[24] R. M. Silverstein, F. X. Webster, Spectrometric Identification of Organic Compounds, 6th ed., John Wiley and Sons, New York, 1998,

[25] Mehmet Eşref Alkış, Kenan Buldurun, Nevin Turan, Yusuf Alan, Ünzile Keleştemur Yılmaz, Asim Mantarcı, Synthesis, characterization, antiproliferative of pyrimidine based ligand and its Ni(II) and Pd(II) complexes and effectiveness of electroporation, Journal of Biomolecular Structure and Dynamics, 40, 9, (2022), 4073-4083 https://doi.org/10.1080/07391102.2020.1852965

[26] Xubiao Luo, Haiyan Yu, Yu Xi, Lili Fang, Lingling Liu, Jinming Luo, Selective removal Pb(II) ions form wastewater using Pb(II) ion-imprinted polymers with bi-component polymer brushes, RSC Advances, 7, 42, (2017), 25811-25820 https://doi.org/10.1039/C7RA03536E

[27] Shanling Hu, Xiaodong Xiong, Shuiying Huang, Xiaoqi Lai, Preparation of Pb(II) Ion Imprinted Polymer and Its Application as the Interface of an Electrochemical Sensor for Trace Lead Determination, Analytical Sciences, 32, 9, (2016), 975-980 https://doi.org/10.2116/analsci.32.975

[28] Hongxing He, Qiang Gan, Changgen Feng, Preparation and application of Ni(II) ion-imprinted silica gel polymer for selective separation of Ni(II) from aqueous solution, RSC Advances, 7, 25, (2017), 15102-15111 https://doi.org/10.1039/C7RA00101K

[29] Morlu Stevens, Bareki Batlokwa, Selective and Simultaneous Removal of Ni (II) and Cu (II Ions from Industrial Wastewater Employing a Double Ni-Cu-Ion Imprinted Polymer, The International Journal of Advanced Engineering Research and Science 5, 6, (2018), 264172 https://dx.doi.org/10.22161/ijaers.5.6.36

[30] Ebrahim Ahmadi, Hassan Hajifatheali, Zeinab Valipoor, Mohamadreza Marefat, Synthesis, characterization and analytical applications of Ni(II) ion-imprinted polymer prepared by N-(2-hydroxyphenyl)acrylamide, Journal of Polymer Research, 28, 5, (2021), 181 https://doi.org/10.1007/s10965-021-02542-w

[31] Ali Khedri, Dariush Jafari, Morteza Esfandyari, Adsorption of Nickel(II) Ions from Synthetic Wastewater Using Activated Carbon Prepared from Mespilus germanica Leaf, Arabian Journal for Science and Engineering, 47, 5, (2022), 6155-6166 https://doi.org/10.1007/s13369-021-06014-7

[32] Zhiyong Zhou, Delong Kong, Huiying Zhu, Nian Wang, Zhuo Wang, Qi Wang, Wei Liu, Qunsheng Li, Weidong Zhang, Zhongqi Ren, Preparation and adsorption characteristics of an ion-imprinted polymer for fast removal of Ni(II) ions from aqueous solution, Journal of Hazardous Materials, 341, (2018), 355-364 https://doi.org/10.1016/j.jhazmat.2017.06.010

[33] Nurhasni Nurhasni, Hendrawati Hendrawati, Nubzah Saniyyah, Penyerapan ion logam Cd dan Cr dalam air limbah menggunakan sekam padi, Jurnal Kimia Valensi, 1, 6, (2010), 310-318 https://doi.org/10.15408/jkv.v1i6.244

[34] Weiye Zhang, Xiujun Deng, Siqing Ye, Yan Xia, Lingling Li, Weili Li, Hongxing He, Selective removal and recovery of Ni(II) using a sulfonic acid-based magnetic rattle-type ion-imprinted polymer: adsorption performance and mechanisms, RSC Advances, 12, 53, (2022), 34571-34583 https://doi.org/10.1039/D2RA06918K

[35] Yuvaraja Gutha, Venkata Subbaiah Munagapati, Mu. Naushad, Krishnaiah Abburi, Removal of Ni(II) from aqueous solution by Lycopersicum esculentum (Tomato) leaf powder as a low-cost biosorbent, Desalination and Water Treatment, 54, 1, (2015), 200-208 https://doi.org/10.1080/19443994.2014.880160

[36] Mehrnoush Mohammadi, Ahad Ghaemi, Meisam Torab-Mostaedi, Mehdi Asadollahzadeh, Alireza Hemmati, Adsorption of cadmium (II) and nickel (II) on dolomite powder, Desalination and Water Treatment, 53, 1, (2015), 149-157 https://doi.org/10.1080/19443994.2013.836990

[37] Rajeswari M. Kulkarni, K. Vidya Shetty, G. Srinikethan, Cadmium (II) and nickel (II) biosorption by Bacillus laterosporus (MTCC 1628), Journal of the Taiwan Institute of Chemical Engineers, 45, 4, (2014), 1628-1635 https://doi.org/10.1016/j.jtice.2013.11.006

[38] Zihong Cheng, Wei Ma, Lianlian Gao, Zhanxian Gao, Ren Wang, Jun Xu, Gang Xin, Adsorption of nickel ions from seawater by modified chitosan, Desalination and Water Treatment, 52, 28-30, (2014), 5663-5672 https://doi.org/10.1080/19443994.2013.841107

[39] Yong Dai, Shengmao Zhao, Ruyi Zheng, Adsorption and removal of pentavalent antimony from water by biochar prepared from modified rosa roxburghii residue, Frontiers in Environmental Science, Volume 12 - 2024, (2025), 1540638 https://doi.org/10.3389/fenvs.2024.1540638

[40] Bhavika Garg, Palkaran Sethi, Soumen Basu, Strategic innovation in CuBTC/PANI nanocomposites for dye remediation: a holistic approach for enhancing adsorption, isotherms, and kinetic studies, RSC Sustainability, 3, 5, (2025), 2311-2324 https://doi.org/10.1039/D5SU00056D